ORIGINAL PAPER

RNA-seq Analysis Reveals Ethylene-Mediated Reproductive Organ Development and Abscission in Soybean (*Glycine max* L. Merr.)

Yun-Qing Cheng · Jian-Feng Liu · Xiangdong Yang · Rui Ma · Chunming Liu · Qiang Liu

Abstract The high level of abscission of developing reproductive organs in soybean (*Glycine max* L. Merr.) causes severe yield loss. The role of ethylene in hastening organ abscission has been well documented. However, little is known about the regulatory mechanism by which ethylene influences abscission in soybean. Ethylene synthesis inhibitor [0.5 mM silver thiosulfate (STS)], ethylene-releasing compound [400 mg/L ethephon (ETH)], and water were applied twice with a 5-day interval between the applications. The STS-treated plants produced more flowers and pods, resulting in 55.6 % greater seed yield. ETH treatment significantly increased ($P<0.05$) the abscission rate of flowers and pods. Three digital gene expression libraries (STS-, ETH- and control library) were constructed. Illumina sequencing of the three libraries was used to identify 9.7 to 10.5 million unigenes. Strong correlations were observed among different gene expression profiles and specific metabolite groups (such as plant hormone biosynthesis and signal transduction; starch and sucrose metabolism; and secondary metabolism) suggesting the importance of these metabolic pathways during ethylene regulation. Potential ethylene target genes such as *1-aminocyclopropane-1-carboxylate (ACC)-oxidase, 2C protein phosphatases (PP2Cs), MAT1, acetyltransferase, bidirectional sugar transporter SWEET1-like*, and so on were identified. These results suggest that ethylene regulates flower and pod abscission in soybean by direct transcriptional regulation of genes that are involved in the metabolic and regulatory processes related to both floral organ development and abscission. Thus, these findings further elucidate the critical role of ethylene in transcriptional regulation of reproductive organ development and abscission.

Keywords Abscission · Development · Reproductive organ · RNA-Seq analysis · Soybean

Introduction

Soybean (*Glycine max* L. Merr.) plants develop numerous flowers and pods. However, under field conditions, most of the flowers and young pods abscise rather than develop into mature pods. The abscission of flowers and pods is the primary cause of yield loss in soybean (Heindl and Brun 1984; Rylott and Smith 1990). The abscission percentage ranges from 67 % to 82 % across different soybean cultivars (Wiebold et al. 1981). Biotic (insect and microbial infection) and abiotic (temperature changes, drought, salinity) stresses can influence abscission of soybean flowers and young pods. Ethylene is a hormone involved in early senescence and abscission of vegetative and reproductive organs under stress conditions (Xue et al. 2008). However, the metabolic network triggered by ethylene during organ abscission is not well understood (Singh et al. 2011). Genome-wide gene expression profiles of insertional mutants can help elucidate the relationship between gene function and plant development (Hirayama and Shinozaki 2010). However, no organ abscission mutants have been identified in soybean. In addition, a major challenge faced by scientists in the field of functional genomics is the prevalence of gene families (Alonso and Ecker 2006; Stangeland et al. 2005) with family members that encode proteins with redundant functions (Gu et al. 2003;

Y.-Q. Cheng · J.-F. Liu (✉) · C. Liu · Q. Liu
College of Life Sciences, Jilin Normal University,
Siping, Jilin 136000, People's Republic of China
e-mail: jianfengliu1976@163.com

X. Yang · R. Ma
Agro-Biotechnology Research Institute,
Jilin Academy of Agricultural Sciences,
Changchun, Jilin 130024, People's Republic of China

Pasek et al. 2006). Due to the presence of gene-families with a functional redundancy it is often the case that mutations of a gene will not display any detectable phenotype (Kubis et al. 2004). To overcome this problem, the physiological effect of ethylene was previously characterized by employing precursors/inhibitors involved in ethylene biosynthesis or signaling (Nambeesan et al. 2012; Trivellini et al. 2011; Lin et al. 2009; Schaller 2012).

Ethylene biosynthesis starts with the conversion of S-adenosyl-L-methione (SAM) into 1-aminocyclopropane-1-carboxylic acid (ACC) catalyzed by the enzyme 1-aminocyclopropane-1-carboxylate synthase (ACS). ACC can then be converted to either 1-(malonylamino) cyclopropane-1-carboxylic acid (MACC) by ACC N-malonyl transferase, or to the end product, ethylene, by 1-aminocyclopropane-1-carboxylate oxidase (ACO; Adams and Yang 1979). The success in molecular cloning of ACS and ACO (Sato and Theologis 1989; Hamilton et al. 1991) genes suggests that these enzymes belong to multigene families and are regulated by developmental and environmental stimuli. Ethylene targets a family of membrane-localized receptors, which actively repress ethylene responses. The key elements in ethylene signaling pathway include Raf-like kinase constitutive triple response-1 (CTR1), transmembrane protein EIN2 (ethylene insensitive 2), and the EIN3 (ethylene insensitive 3)-like family of transcription factors (Schaller 2012). Ethylene binding to its receptors relieves the repression on downstream signaling components that results in the activation of EIN3-like transcription factors, which initiate the transcriptional response to ethylene. Ethylene induces genes encoding several other families of transcription factors, such as the ethylene response factor (ERF) and ethylene response DNA-binding factor (EDF) families, indicating that a transcriptional cascade acts downstream of the EIN3-like proteins (Schaller 2012; Dong et al. 2010). On the basis of this knowledge, some inhibitors and inducers of ethylene synthesis and action have been used to study the function of ethylene on plant growth and development. The pharmacological agent aminoethoxyvinylglycine (AVG) and silver can be used to inhibit ethylene responses through their ability to target ethylene biosynthesis or ethylene receptors, respectively (Schaller 2012). Ethephon (ETH) is an ethylene-releasing compound that can release ethylene in the presence of water at a pH above 3.5 (Lorbiecke and Sauter 1999). Typically, either ETH or the ethylene precursor ACC is employed to induce ethylene production (Zhang and Wen 2010).

Genome-wide gene profiling techniques are evolving rapidly. A combination of ethylene inhibitor/inducer and genome-wide gene expression profiling may help to reveal the complicated physiological networks triggered by ethylene in organ abscission in soybean. RNA-Seq is a recently developed approach for transcriptome profiling and is enabled by deep-

sequencing technologies to provide a far more precise measurement of the levels of transcripts and isoforms than those provided by other methods (Wang et al. 2009). The holistic view of the transcriptome and its organization provided by the RNA-Seq method reveals many novel transcribed regions, splice isoforms, single nucleotide polymorphisms (SNPs), and the precise location of transcription boundaries (Cloonan and Grimmond 2008; Li et al. 2008; Lister et al. 2008; Wilhelm et al. 2008). RNA-Seq generates absolute, rather than relative, gene expression measurements, providing greater insight and accuracy than microarrays (Hoen et al. 2008; Marioni et al. 2008; Mortazavi et al. 2008). For example, Illumina sequencing technology offers millions of sequence reads from a single instrument run and thereby permits gene expression profiling experiments with an improved dynamic range and considerable cost savings (Xue et al. 2010).

To better understand the role of ethylene in regulating organ abscission in soybean, the RNA-Seq technique was used to elucidate the regulatory network triggered by ethylene. Genome-wide comparative transcriptome analysis was conducted using RNA from three treatments: (1) distilled water (control), (2) STS treatment (inhibitor of ethylene action), and (3) ETH treatment (ethylene releaser). The digital gene expression (DGE) libraries for each of the three treatments were constructed by the RNA-seq method and compared to identify the regulatory network involved in ethylene-mediated abscission of developing reproductive organs in soybean.

Materials and Methods

Plant Materials and Experimental Design

In 2011, soybean (cv. Tiefeng-31) was planted in a greenhouse under irrigated conditions in Jilin Normal University, Siping, Jilin province, China. On 2 May (21–29 °C), four seeds were planted per pot (7.6 L) and two plants were selected after 14 days. Twenty-four replicate pots per treatment were arranged in a completely randomized block design. At the beginning bloom-R1 stage (Fehr et al. 1971), plants (in their entirety) were sprayed with 0.5 mM STS or 400 mg/L ETH dissolved in distilled water twice with a 5-day interval between applications. The control plants were sprayed with distilled water. It is known that plants often increase ethylene production in response to environmental stress (Djanaguiraman et al. 2011). Additionally, it has been reported previously that when stress occurs at the flowering (R1 and R2), or early pod development (R3 and R4) stage, the pod number is reduced because of high abscission rate of flower and pod (Heindl and Brun 1984; Hirayama and Shinozaki 2010). To obtain complete gene-expression data of flower- and pod-development stages, a total of nine plants

(three from each treatment: STS, ETH, and distilled water) were randomly selected, following which the auxiliary buds and surrounding node tissue (third node from the top) were dissected separately on days 0, 7, 14, 21, 28, and 35 (from R1 to R4 stage) after the second spraying. The plant samples were quickly frozen in liquid nitrogen and stored at −80 °C and later used for RNA extraction. The three remaining replicate pots were used to estimate the pod number by recording the abscission rate of flowers and pods during the reproductive stage and to measure the dry matter weight of the seeds and the straw at harvest. The numbers of flowers and pods were determined by artificial counting. Just before flower initiation, four plants from each treatment set were selected randomly and tagged for subsequent flower and pod counting. All emerging flower buds were marked and counted with an oil-based pen. The sepals were marked to avoid a repeat count in subsequent visits, which occurred at 2-day intervals. Flowers and pods on the stem were also counted. Pod location was counted every 2 days by touching the tips of all the young pods, which were not less than 2 cm long, with an oil-based pen. Percent flower and pod abscission were counted every 7 days. Percent of flower and pod abscission at different stages = number of flowers and pods with abscission × 100 %/(number of flowers and pods with abscission + the number of flowers and pods retained on the plant).

RNA Extraction

Total RNA of every sample was extracted from the dissected tissue using the RNA Easyspin Isolation System (Aidlab Biotech, Beijing, China) and treated with RNase-free DNase to eliminate the residual genomic DNA. All steps were followed according to the manufacturer's instructions (Promega, Beijing, China). Total RNA was then quantified using a spectrophotometer and loaded on a denaturing agarose gel to check RNA concentration and integrity.

DGE Library Preparation and Sequencing

Total RNA was isolated from samples collected at different developmental stages. Equal amounts of RNA from each developmental stage were mixed to make a total RNA pool for library preparation and sequencing. Three pools of mRNA samples, one representing each treatment, were used to build libraries. Total mRNA was enriched using the oligo (dT) magnetic beads. Fragmentation buffer, which fragments the mRNA into short fragments (about 200 bp), was added. First strand cDNA was synthesized using random hexamer-primers, and the mRNA fragments were used as templates. Buffer, dNTPs, RNase H, and DNA polymerase I were added to synthesize the second strand. Double stranded cDNA was purified with QiaQuick PCR extraction kit and washed with EB buffer for end repair and single nucleotide A (adenine)

addition. Finally, sequencing adaptors were ligated to the fragments. The required fragments were purified by agarose gel electrophoresis and enriched by PCR amplification. The library products were then ready for sequencing analysis using Illumina HiSeq™ 2000 (http://www.illumina.com).

Digital gene expression (DGE) tags were mapped by sequencing raw reads and filtering them to remove: (1) reads with adaptors, (2) reads in which unknown bases were more than 10 %, and (3) low quality reads. [50 % of the read had low quality bases (quality value, ≤5).] For tag annotation, the clean reads were mapped to reference sequences using SOAPaligner/soap2 (Li et al. 2009). Mismatches of no more than two bases were allowed in the alignment. The clean tags were designated as unambiguous clean tags. The gene expression was calculated by the number of reads mapped to the reference sequence and every gene.

Screening of Differentially Expressed Genes

To compare the differences in gene expression, the tag frequency in each differentially expressed gene (DGE) library was analyzed statistically according to the method described by Audic and Claverie (1997). A strict algorithm was used to identify DEGs between two samples. If x denotes the number of unambiguous clean tags from gene A, then, given that every gene's expression occupies only a small part of the library, $p(x)$ will closely follow the Poisson distribution.

$$p(\mathrm{x}) = \frac{e^{-\Lambda}\Lambda^x}{x!} \ (\Lambda \text{ is the real transcript of the gene})$$

If the total number of clean tags in sample 1 is N1, and the total number of clean tags in sample 2 is N2; gene A holds x tags in sample 1 and y tags in sample 2, then the probability of gene A expressed equally between two samples can be calculated by the following equation:

$$2\sum_{i=0}^{i=y} p(i|\mathrm{x}) \text{ or } 2 \times \left(1 - \sum_{i=0}^{i=y} \mathrm{p}(i|\mathrm{x})\right)\left(\text{if} \sum_{i=0}^{i=y} \mathrm{p}(i|\mathrm{x}) > 0.5\right)$$

$$p(y|x) = \left(\frac{N2}{N1}\right)^y \frac{(x+y)!}{x!y!\left(1 + \frac{N2}{N1}\right)^{(x+y+1)}}$$

The P-value corresponds to the differential gene expression test. False discovery rate (FDR) is a method used to determine the threshold of P-value in multiple tests. Assume that we identified R DEGs in which S genes really show differential expression and the other V genes are false positive. If we decide that the error ratio "$Q = V/R$" must stay below a cutoff (e.g., 1 %), we should preset the FDR to a number no larger than 0.01 (Benjamini and Yekutieli 2001).

We use "FDR≤0.001 and the absolute value of log₂Ratio≥ 1" as the threshold to judge the significance of gene expression difference. More stringent criteria with smaller FDR and bigger fold-change value can be used to identify DEGs. The DEGs were used for gene ontology (GO) enrichment analyses.

GO Analysis of DEGs

Gene ontology enrichment analysis provides all GO terms that were significantly enriched in the DEGs as compared to those in the genome background, and filters the DEGs that correspond to biological functions. This method can be used to: (1) map all the DEGs with the GO terms in the database (http://www.geneontology.org/), (2) calculate gene numbers for every term, (3) find significantly enriched GO terms in DEGs as compared to those in the genome background by using hypergeometric test.

The calculation formula is:

$$P = 1 - \sum_{i=0}^{m-1} \frac{\binom{M}{i}\binom{N-M}{n-i}}{\binom{N}{n}}$$

In the equation, N is the number of all genes with GO annotation; n is the number of DEGs in N; M is the number of all genes that are annotated to the certain GO terms; m is the number of DEGs in M. The calculated P-value goes through Bonferroni correction, taking corrected P-value≤ 0.05 as a threshold. GO terms fulfilling this condition are defined as significantly enriched GO terms in DEGs. Using this analysis, we were able to recognize the main biological functions of DEGs. The GO functional enrichment analysis enabled us to integrate the cluster analysis of expression patterns.

Pathway Enrichment Analysis of DEGs

Genes commonly interact with each other and these interactions can play crucial roles in certain biological functions (Amit et al. 2009). Pathway-based analysis helps to further understand biological functions of genes. KEGG is the major public pathway-related database (Kanehisa et al. 2008). Pathway enrichment analysis identifies significantly enriched metabolic pathways or signal transduction pathways in DEGs compared to those in the whole genome background. The calculating formula is the same as that in GO analysis. Here N is the number of all genes with KEGG annotation, n is the number of DEGs in N, M is the number of all genes annotated to specific pathways, and m is number of DEGs in M.

Validations of RNA-Seq Data by RT-qPCR

Real-time quantitative PCR (RT-qPCR) was performed to validate the RNA-Seq results for ethylene-responsive gene transcripts, whose change in tissues treated by ETH treatment was in the opposite direction to that in STS-treated tissues. Total RNA was extracted and pooled as described for DGE library preparation. At least two independent biological replicates of each treatment and three technical replicates of each biological replicate were used for the RT-PCR analysis. We used 100 ng total RNA for reverse transcription to cDNA using the PrimeScript RT reagent Kit (TaKaRa, Tokyo, Japan) in a 10-µL reaction mixture containing 1× PrimeScript buffer, 50 pmol random 6-mer primer, and 0.5 µL PrimeScript RT Enzyme Mix I. RT-qPCR was performed with 1 µL cDNA template, 1× reaction buffer, 0.2 mM dNTP mixture, 0.4 µM each primer, 0.6× SYBR Green I dye (Generay Biotech), and 0.3 units of r*Taq* DNA polymerase (TaKaRa) in a Rotor-Gene 2000 thermocycler (Corbett Research, Sydney, Australia) and analyzed using Rotor-Gene Real-Time Analysis Software 6.0 Build 14 (Corbett Research, Mortlake, Australia). Melting curves for each PCR were monitored carefully to avoid nonspecific amplifications. The results were normalized to the expression level of the constitutive *β-tubulin* gene. A relative quantitative method was used to evaluate the quantitative variation. The Primers used in RT-qPCR study are shown in Table 1.

Results

Effects of STS and ETH on Growth and Development in Soybean

There were significant differences in vegetable growth and reproductive development of soybean among the three treatments (Table 2, Fig. 1). Dry weight of seed and straw at harvest was promoted by STS and reduced by ETH treatment. Plants treated with STS produced more flowers and pods and their seed yield increased by 55.6 % compared with the control. ETH treatment promoted the abscission ratio of flowers and pods significantly ($P<0.05$), and the data indicated that ETH might have long-lasting negative effects on flower and pod development. STS treatment did not affect the abscission of flowers and pods significantly ($P<0.05$). More lateral branches were observed at the base of fruit branch after ETH treatment (Fig. 1), and STS distinctly suppressed branching growth as compared to that of control and ETH treatment.

Illumina Sequencing and Sequence Mapping

Three cDNA libraries were generated from a mixture of RNA isolated from buds and surrounding node tissue from the third

Table 1 Primers used in real-time quantitative PCR (RT-qPCR)

Gene ID	Gene	Forward primer sequence (5′-3′)	Reverse primer sequence (5′-3′)	Length (bp)
547615	Soybean clone JCVI-FLGm-19A20	CCTGCAGCCACTTCCCGAGC	TGCCTGCAGTGATCAATTTGGGAG	133
547829	MAT1 maturation-associated protein	GGGGTGCGCACACTGAAGCA	GCATGCACGATGCATCTACTTGTCA	149
100305883	JCVI-FLGm-2L15 unknown mRNA	CCAAGGCCCAAGCAGCAGTGA	ATTGCAGCAAGGGCCAGGCA	107
100306032	*Glycine max* uncharacterized LOC100306032	CTGCTTGTGAGGGTTGCCAGC	ACACCTCCACCAGGACCCCT	152
100500612	*Glycine max* uncharacterized protein LOC100500612	CCCGAAACCATGGAGGCGCT	GCATGACGTGACCATGCGAGC	129
gnl|UG|Gma#S39303376	GLLBG53TF JCVI-SOY1	GGAGCAGGAACCGCAACAGGA	ACACTTCCACCACTGCCGGG	122
gnl|UG|Gma#S47723140	*Glycine max* cDNA clone GMFL01-14-L06	CCACCCAAATGTTGCTCGCCCA	GCTGAGTGGAAGGTTGAAGGGGC	93
gnl|UG|Gma#S48312502	*Glycine max* probable protein phosphatase 2C 58-like	GGGCGAGGAGGGTCAACAGC	AACCCCCACGCCTCTCAATCG	172
gnl|UG|Gma#S48316018	*Glycine max* probable mannitol dehydrogenase-like	GCCACTCGGACCTCCACAGC	GGCAGGTGCGGCAGGAATCA	171
gnl|UG|Gma#S4992524	*Glycine max* cDNA clone Gm-r1070-5150	CCACCACTGCCAGGGTTTGGA	TTGGGGGAGTAGGGCTGCCA	166
gnl|UG|Gma#S53085092	JCVI-FLGm-23O16	GCACAGGAGACAGAGCAAGTGTACC	GGCTTGAAATCTTGGCTCCTTTGGC	102
gnl|UG|Gma#S53085474	Soybean clone JCVI-FLGm-16L19	TGCCTCTCCTCTTCGGCCAT	ACACACTACACACACTCCCCTCA	118
gnl|UG|Gma#S53085706	JCVI-FLGm-12C20	GGCCAAGTCCCCAGGCTTACC	GCACTGGTGGAGCAGTGGCTT	114
gnl|UG|Gma#S53086117	JCVI-FLGm-16M16	TGGGACCAGAATGTCCGTAGCCT	CCCAACAATGCTGGTGCAGGGT	78
gnl|UG|Gma#S53087057	Soybean clone JCVI-FLGm-21I20	TTGGGAGCTTTCAAGACCGTGAC	ACAACTGCTCCCATGGCTGTGT	128
gnl|UG|Gma#S53087628	JCVI-FLGm-9P19	GCGCATTCCAATGCACAGAACGG	TGCAAGTGTGCTTGGGTTACCG	98
gnl|UG|Gma#S53088986	JCVI-FLGm-6F15	AGCCTTTTCCTTCCTTGGTGCC	TGGTTTGCCTTTTGTGTTTCCCCA	121
547976	ACC synthase	CACCTCAAATCCCGGTCAA	AGCAACTGGAGCACACGAAG	105
gnl|UG|Gma#S5042179	β-Tubulin	TCTCGTCCATCCCCTCCCCAGTG	GTTTAGGAGGGTCAGCGAGCAGTTC	84

nodes from the apex of the plants, for each of the three treatments. After filtering the low quality tags, the total number of clean tags in each library ranged from 11 to 12 million (Table 3), and the percentage of clean tags among the raw tags in each library ranged from 99.54 % to 99.56 % (Supplement file 1). Reads that failed to meet these criteria or mapped to multiple locations were excluded. Among the clean tags, the number of sequences that could be mapped to unigenes ranged from 9.7 to 10.5 million, and the percentage of these clean tags ranged from 82.8 to 83.7 % in the three libraries (Table 3).

Comparative analysis of the STS and ETH treatment libraries revealed significant expression changes in 1,524 genes. Among these genes, 1,002 up-regulated and 522 down-regulated genes were identified in the STS library as compared to those in the ETH library (Fig. 2). Compared with the control treatment, only 522 DEGs were regulated by STS treatment, but 1,043 DEGs were regulated by ETH treatment. In order to gain further insight into ethylene-regulated target genes during soybean reproductive development, the genes whose expression changes in opposite

Table 2 Effects of silver thiosulfate (STS) and ethephon (ETH) on straw weight, pod number, flower and pod abscission ratio and yield of soybean. Different lower case letters within the same column indicates significant at 0.05 level by Duncan test. *CK* Control

Treatment	Flower and pod abscission rate after different days of treatment (%)					Pod number plant^{-1}	Seed dry yield (g plant^{-1})	Straw dry weight (g plant^{-1})
	0–7	8–14	15–21	22–28	29–35			
CK	21.81±1.66 b	46.02±1.28 b	46.99±2.54 b	35.41±1.33 b	54.39±1.89 b	56.02±3.44 b	46.36±2.55 b	25.14±1.27 b
STS (0.5 mM)	13.75±0.84 b	33.18±2.17 b	40.88±5.24 b	49.52±1.78 a	51.34±2.88 b	53.25±3.01 b	60.24±5.85 a	39.12±1.83 a
ETH (400 mg L^{-1})	95.84±4.87 a	80.67±3.45 a	72.34±2.49 a	14.58±0.52 c	76.23±3.84 a	80.26±3.91 a	24.13±0.97 c	7.89±0.35 c

directions in control-VS-STS and control-VS-ETH DEGs were chosen as the direct ethylene-responsive genes (Table 4).

GO Classification

GO assignments were used to classify the functions of the predicted ethylene regulative genes. Based on DEGs, 2,571 differentially expressed sequences from all the three treatments can be categorized into 28 functional groups (Fig. 3). In each of the three main categories (biological process, cellular component and molecular function) of GO classification, 'response to stimulus', 'external encapsulating structure' and 'catalytic activity' terms are dominant in the DEGs, respectively. In the control-vs-STS treated samples, a high-percentage of genes that showed change in expression belonged to the category of 'molecular function', and a smaller number of genes that showed expression changes belonged to the 'biological process' category (Fig. 3). DEGs did not show a difference in expression in the 'cellular component' category of the control-vs-ETH library. The GO analysis showed that the functions of the 17 ethylene-responsive genes were involved mainly in the various stimulus responses and catalytic activities, which may in turn be involved in the ethylene-mediated response.

Table 3 Alignment statistics of map to gene and genome

| Treatment	Map to gene	Read number	Percentage	Map to genome	Read number	Percentage
STS	Total reads	12099809	100.00 %	Total reads	12099809	100.00 %
	Total base pairs	592890641	100.00 %	Total base pairs	592890641	100.00 %
	Total mapped reads	7877984	65.11 %	Total mapped reads	10057755	83.12 %
	Perfect match	6191302	51.17 %	Perfect match	9029649	74.63 %
	<=2 bp mismatch	1686682	13.94 %	<=3 bp mismatch	1028106	8.50 %
	Unique match	6601419	54.56 %	Unique match	8637620	71.39 %
	Multi-position match	1276565	10.55 %	Multi-position match	1420135	11.74 %
	Total unmapped reads	4221825	34.89 %	Total unmapped reads	2042054	16.88 %
Control	Total reads	12467552	100.00 %	Total reads	12467552	100.00 %
	Total BasePairs	610910048	100.00 %	Total BasePairs	610910048	100.00 %
	Total mapped reads	8158445	65.44 %	Total mapped reads	10443531	83.77 %
	Perfect match	6404180	51.37 %	Perfect match	9363251	75.10 %
	<=2 bp mismatch	1754265	14.07 %	<=3 bp mismatch	1080280	8.66 %
	Unique match	6862615	55.04 %	Unique match	9005205	72.23 %
	Multi-position match	1295830	10.39 %	Multi-position match	1438326	11.54 %
	Total unmapped reads	4309107	34.56 %	Total unmapped reads	2024021	16.23 %
ETH	Total reads	11783476	100.00 %	Total reads	11783476	100.00 %
	Total BasePairs	577390324	100.00 %	Total BasePairs	577390324	100.00 %
	Total mapped reads	7363034	62.49 %	Total mapped reads	9757392	82.81 %
	Perfect match	5760539	48.89 %	Perfect match	8753428	74.29 %
	<=2 bp mismatch	1602495	13.60 %	<=3 bp mismatch	1003964	8.52 %
	Unique match	6248261	53.03 %	Unique match	8374964	71.07 %
	Multi-position match	1114773	9.46 %	Multi-position match	1382428	11.73 %
	Total unmapped reads	4420442	37.51 %	Total unmapped reads	2026084	17.19 %
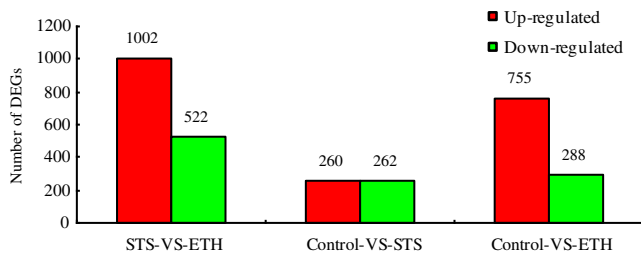
Fig. 2 Changes in gene expression profile among the different treatments. *DEGs* Differentially expressed genes

Pathway Enrichment Analysis of DEGs

Ethylene-affected biological pathways were evaluated by enrichment analysis of DEGs. Significantly enriched metabolic pathways and signal transduction pathways were identified. Pathways with a Q value<0.05 were significantly enriched. DEGs with pathway annotation after ETH and STS treatment were listed according to enrichment priority (Tables 5, 6). Secondary metabolism (flavone and flavonol biosynthesis, phenylpropanoid biosynthesis, glyoxylate and dicarboxylate metabolism, caffeine metabolism, some hormone metabolism) and primary metabolism (limonene and

pinene degradation, ABC-transporter-dependent pathways and circadian rhythm–plant–reference pathway) were affected by up-regulated DEGs after ETH treatment. After STS treatment, the up-regulated DEGs affected flavonoid biosynthesis, pentose and glucuronate interconversions, starch and sucrose metabolism and some hormone metabolism pathway. Plant–pathogen interaction, hormone biosynthesis and signal transduction pathways were identified to be enriched and were affected by down-regulated DEGs.

Further analysis of pathways showed that the expression of cysteine synthase and ACC oxidase gene expression was enhanced by ETH treatment, and that ACC syntheses was inhibited by STS treatment in ethylene biosynthesis pathway. Similarly, the other regulated plant-hormone biosynthesis pathways included phenylalanine metabolism, carotenoid biosynthesis, linoleic acid metabolism along with the plant hormone signal transduction pathway (see electronic supplementary material, Supplementary files 2, 3). The up-regulated DEGs of control-vs-STS related to plant hormone biosynthesis and signal transduction pathway were plant hormone auxin, cytokine, brassinosteroid and salicylic acid, while the down-regulated DEGs included genes involved in the biosynthesis process of plant hormone gibberellin, abscisic acid, ethylene and jasmonic

Table 4 Genes with opposite expression profiles in Control-vs-STS and Control -vs- ETH differentially expressed genes (DEGs) in soybean

| Gene ID	STS expression	Control expression	ETH expression	log2 Ratio (STS/control)	log2 Ratio (ETH/control)	Functional annotation
547615	23.7193	10.03045	2.058061	1.241674567	−2.285028097	Anthocyanidin synthase
547829	10.4525	22.96056	51.09558	−1.1353164	1.154040264	MAT1, maturation protein
100305883	115.9152	7.832034	2.037342	3.88753952	−1.94269881	Non-specific lipid-transfer protein
100306032	158.9021	15.6621	1.959729	3.342788551	−2.998552045	Non-specific lipid-transfer protein
100500612	7.150735	17.73947	68.78933	−1.31080008	1.955222085	Uncharacterized acetyltransferase At3g50280
gnl|UG|Gma#S39303376	356.5335	130.8056	24.67008	1.446613412	−2.406590077	Aconitate hydratase
gnl|UG|Gma#S47723140	156.6997	54.1286	10.43341	1.533539501	−2.375180583	Anthocyanidin synthase
gnl|UG|Gma#S48312502	8.8375	21.91144	59.83588	−1.30997047	1.449326599	Probable protein phosphatase 2C 58-like
gnl|UG|Gma#S48316018	5.9856	13.06581	42.32181	−1.12622108	1.695604148	Cinnamyl alcohol dehydrogenase
gnl|UG|Gma#S4992524	36.7375	17.66963	3.024464	1.05598225	−2.546520338	Putative cell wall proteins, which are usually associated with different abiotic and biotic stress conditions
gnl|UG|Gma#S53085092	2.7520	7.580656	17.97362	−1.46186606	1.24548662	1-aminocyclopropane-1-carboxylate oxidase-li
gnl|UG|Gma#S53085474	21.7088	9.827072	2.529682	1.143445091	−1.957805703	Probable caffeoyl-CoA O-methyltransferase At4g26220-like
gnl|UG|Gma#S53085706	19.9483	8.395221	2.799133	1.248627328	−1.584588379	Glutathione S-transferase F11-like
gnl|UG|Gma#S53086117	13.6225	53.25486	118.479	−1.96691815	1.153646282	*Vigna angularis* mRNA for ACC-oxidase
gnl|UG|Gma#S53087057	30.9698	66.15091	154.3541	−1.0949003	1.222410425	*Glycine max* glucan endo-1,3-beta-glucosidase 14-like
gnl|UG|Gma#S53087628	11.2783	26.80343	96.96129	−1.24887233	1.854991305	Uncharacterized protein LOC100782360 precursor
gnl|UG|Gma#S53088986	24.8864	8.326688	3.048467	1.579544206	−1.449658799	Bidirectional sugar transporter SWEET1-like
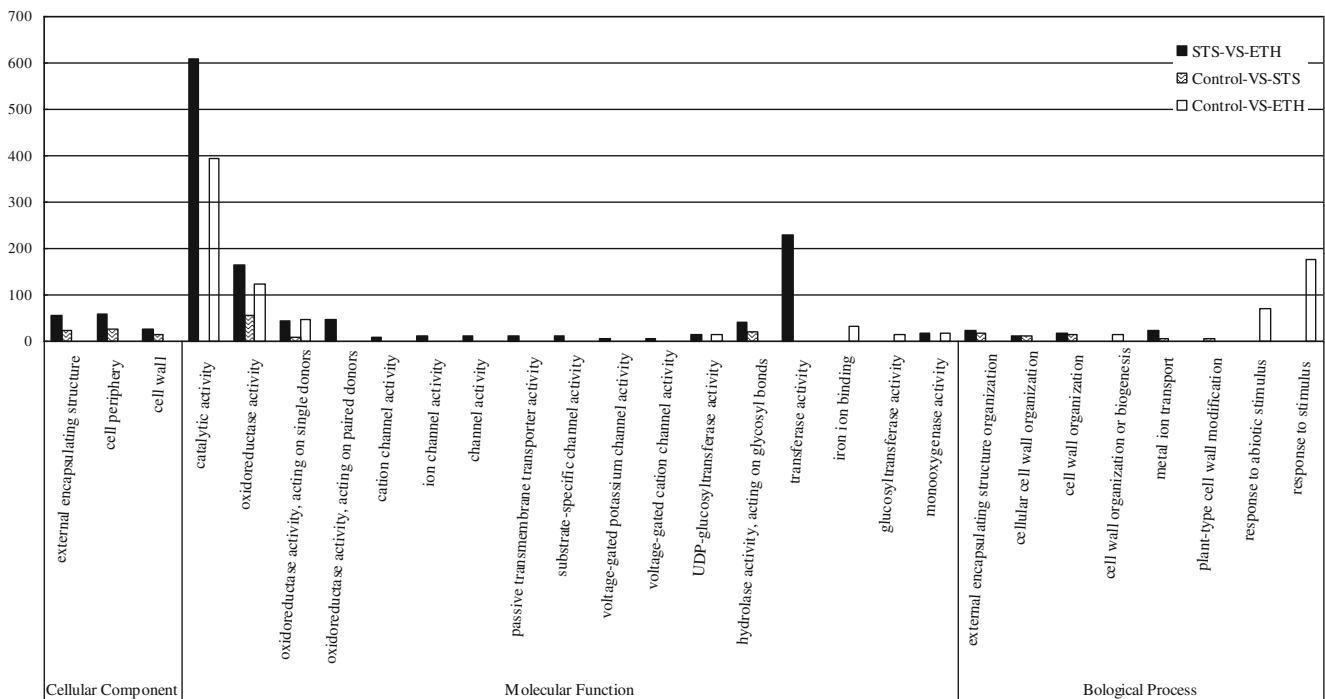
Fig. 3 Gene ontology (GO) categories of unigenes. Unigenes were annotated in three categories: cellular components, molecular functions and biological processes

acid. The ETH treatment had the contrary effects on the biosynthesis and signal transduction pathway of plant hormone auxin, abscisic acid, ethylene, salicylic acid and jasmonic acid. These findings provided clues to unravel the complicated signal networks of phytohormones.

DEG Functional Annotation and RT-qPCR Confirmation

The putative function of the 17 ethylene-responsive genes was determined on the basis of sequence similarity with the genomes of soybean, *Medicago truncatula*, and *Arabidopsis thaliana* using the BLASTN program. In the similarity range, 16 transcripts were classified as "known protein," and only 1 unigene had unknown annotations. The seven up-regulated expression unigenes in ETH treatment included two *ACC-oxidase* genes (gnl|UG|Gma#S53085092, gnl|UG|Gma#S53086117), one central component *PP2Cs* gene of abscisic acid (ABA) signal transduction (gnl|UG|Gma#S48312502), two genes responding to stimulus [maturation protein gene (*MAT1*), and an uncharacterized acetyltransferase gene (*At3g50280*)], *cinnamyl alcohol dehydrogenase* gene (gnl|UG|Gma#S48316018) involved in cell-wall degradation and *Glycine max glucan endo-1, 3-beta-glucosidase 14-like* gene involved in cellulose degradation. The remaining nine up-regulated unigenes in STS treatment and down-regulated genes in ETH treatment included two *anthocyanidin synthase* genes (547615, gnl|UG|Gma#S39303376) and two non-specific *lipid-transfer protein* genes (100305883, 100306032), one *aconitate hydratas* gene (gnl|UG|Gma#S47723140), one putative cell wall protein gene (gnl|

UG|Gma#S4992524), one bidirectional sugar transporter *SWEET1-like* gene (gnl|UG| Gma#S53088986), and one *glutathione S-transferase F11-like* gene (plays a role in plant growth and development in vivo and shoot regeneration in vitro). On the basis of the GO functional classification, the nine up-regulated genes in control-VS-STS treatment were thought to be involved in the biosynthesis of carbohydrate metabolism, translocation, plant growth, and development, and the seven up-regulated genes in control-vs-ETH were involved in ABA and ethylene metabolism, stress stimulus, abscission, ripeness, and senescence processes.

We further analyzed the expression of these 17 responsive genes by RT-qPCR to confirm their gene expression pattern after different treatments. Transcript levels for each of the 17 genes were quantified using SYBR Green technology (Fig. 4), and the results showed good correlation with those obtained by RNA-seq.

Gene Expression Variations During Different Developmental Stages

We also focused on gene expression variations related to ethylene biosynthesis at the reproductive developmental stage. *ACS* and *ACO* gene expression variations were assessed by RT-qPCR (Figs. 5, 6). The results showed that gene expression levels of *ACO* and *ACS* were both low on day 0 and reached their peak value on days 14 and 21 in the control treatment, respectively. The *ACO* gene expression in ETH treatment was significantly higher compared with that

Table 5 Pathway enrichment analysis of control-vs-ETH DEGs

#	Pathway (control-vs-ETH)	DEGs with pathway annotation (491)	All genes with pathway annotation (14,372)	P value	Q value	Pathway ID
1	Biosynthesis of secondary metabolites	123 (25.05 %)	1,876 (13.05 %)	1.99E-13	1.93E-11	ko01110
2	Stilbenoid, diarylheptanoid and gingerol biosynthesis	29 (5.91 %)	204 (1.42 %)	6.83E-11	3.31E-09	ko00945
3	Metabolic pathways	177 (36.05 %)	3,417 (23.78 %)	3.51E-10	1.13E-08	ko01100
4	Flavonoid biosynthesis	28 (5.7 %)	244 (1.7 %)	1.98E-08	4.80E-07	ko00941
5	Limonene and pinene degradation	22 (4.48 %)	165 (1.15 %)	4.61E-08	8.94E-07	ko00903
6	Phenylpropanoid biosynthesis	34 (6.92 %)	421 (2.93 %)	3.09E-06	5.00E-05	ko00940
7	Carotenoid biosynthesis	16 (3.26 %)	150 (1.04 %)	5.46E-05	7.57E-04	ko00906
8	Flavone and flavonol biosynthesis	10 (2.04 %)	66 (0.46 %)	7.48E-05	9.07E-04	ko00944
9	Phenylalanine metabolism	19 (3.87 %)	211 (1.47 %)	0.000116246	1.25E-03	ko00360
10	ABC transporters	9 (1.83 %)	75 (0.52 %)	0.000998628	9.24E-03	ko02010
11	Cysteine and methionine metabolism	14 (2.85 %)	158 (1.1 %)	0.001047879	9.24E-03	ko00270
12	Glutathione metabolism	13 (2.65 %)	145 (1.01 %)	0.001405355	1.14E-02	ko00480
13	Diterpenoid biosynthesis	8 (1.63 %)	69 (0.48 %)	0.002353916	1.76E-02	ko00904
14	Valine, leucine and isoleucine degradation	10 (2.04 %)	103 (0.72 %)	0.002721879	1.89E-02	ko00280
15	Isoquinoline alkaloid biosynthesis	6 (1.22 %)	43 (0.3 %)	0.003213318	2.08E-02	ko00950
16	Anthocyanin biosynthesis	2 (0.41 %)	4 (0.03 %)	0.006676079	3.81E-02	ko00942
17	Caffeine metabolism	2 (0.41 %)	4 (0.03 %)	0.006676079	3.81E-02	ko00232
18	Tyrosine metabolism	9 (1.83 %)	107 (0.74 %)	0.01097067	5.91E-02	ko00350
19	Benzoxazinoid biosynthesis	5 (1.02 %)	44 (0.31 %)	0.01654052	8.44E-02	ko00402
20	Linoleic acid metabolism	6 (1.22 %)	62 (0.43 %)	0.01886302	9.15E-02	ko00591
21	Nitrogen metabolism	8 (1.63 %)	99 (0.69 %)	0.01995604	9.22E-02	ko00910
22	Glycine, serine and threonine metabolism	8 (1.63 %)	101 (0.7 %)	0.0222239	9.80E-02	ko00260
23	Plant hormone signal transduction	47 (9.57 %)	1,024 (7.12 %)	0.02330565	9.83E-02	ko04075
24	Glyoxylate and dicarboxylate metabolism	6 (1.22 %)	68 (0.47 %)	0.02835907	1.10E-01	ko00630
25	Circadian rhythm - plant	13 (2.65 %)	210 (1.46 %)	0.02843037	1.10E-01	ko04712
26	Sesquiterpenoid biosynthesis	1 (0.2 %)	1 (0.01 %)	0.03416365	1.27E-01	ko00909
27	Alanine, aspartate and glutamate metabolism	8 (1.63 %)	113 (0.79 %)	0.03972911	1.43E-01	ko00250
28	Glucosinolate biosynthesis	3 (0.61 %)	24 (0.17 %)	0.04711944	1.63E-01	ko00966

during the corresponding period in the control treatment (FDR≤0.001), but their change dynamics were similar to each other. *ACS* gene expression was inhibited by STS and ETH treatment on days 7 and 14. On days 21–35, *ACS* gene

Table 6 Pathway enrichment analysis of control-vs-STS DEGs

| #	Pathway(control-vs-STS)	DEGs with pathway annotation (248)	All genes with pathway annotation (14,372)	Pvalue	Qvalue	Pathway ID
1	Flavonoid biosynthesis	21 (8.47 %)	244 (1.7 %)	1.469568e-09	9.405235e-08	ko00941
2	Plant-pathogen interaction	41 (16.53 %)	1,009 (7.02 %)	2.252421e-07	7.207747e-06	ko04626
3	Pentose and glucuronate interconversions	14 (5.65 %)	151 (1.05 %)	3.479637e-07	7.423226e-06	ko00040
4	Phenylpropanoid biosynthesis	22 (8.87 %)	421 (2.93 %)	3.951734e-06	6.322774e-05	ko00940
5	Biosynthesis of secondary metabolites	55 (22.18 %)	1,876 (13.05 %)	4.497753e-05	5.757124e-04	ko01110
6	Stilbenoid, diarylheptanoid and gingerol biosynthesis	13 (5.24 %)	204 (1.42 %)	5.467358e-05	5.831849e-04	ko00945
7	Starch and sucrose metabolism	16 (6.45 %)	353 (2.46 %)	0.0004275607	3.909126e-03	ko00500
8	alpha-linolenic acid metabolism	7 (2.82 %)	127 (0.88 %)	0.006484809	5.187847e-02	ko00592
9	Plant hormone signal transduction	27 (10.89 %)	1,024 (7.12 %)	0.01820674	1.294702e-01	ko04075
10	Carotenoid biosynthesis	6 (2.42 %)	150 (1.04 %)	0.04575415	2.928266e-01	ko00906
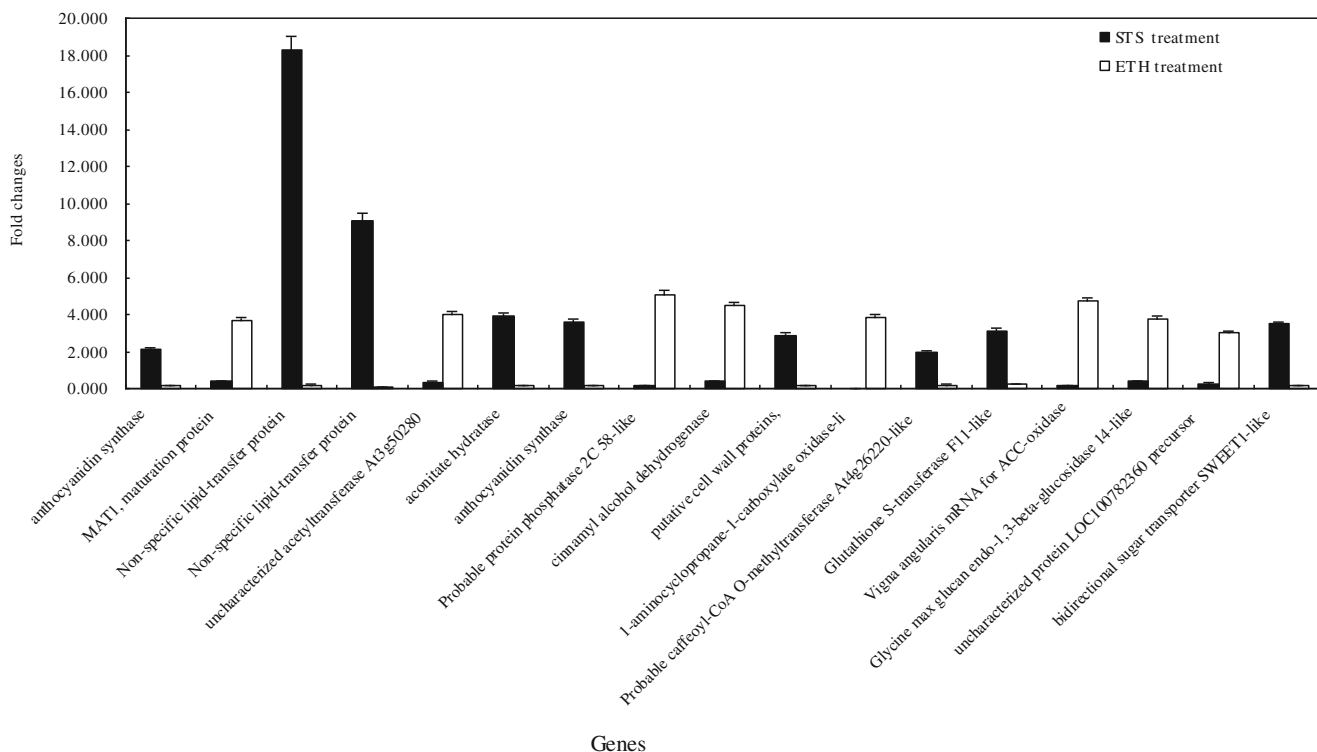
Fig. 4 Expression ratios of 17 genes in STS- or ETH- compared with the control-treatment. β-tubulin RT-qPCR was used as an endogenous control

expression was inhibited by STS treatment and promoted by ETH treatment.

Discussion

Ethylene is a hormone involved in the senescence and abscission of vegetative and reproductive organs under stress conditions. Our results showed that application of

STS at the R1 stage promoted seed yield significantly ($P<$ 0.05), as indicated by the increased flower and pod number (Table 2); a similar phenomenon was observed previously by Chen et al. (2011). Aminoethoxyvinylglycine and 1-methylcyclopropene—two ethylene perception inhibitors—were both beneficial for flower-bud and pollen formation due to the enhanced photosynthetic rate of source leaves (Cheng et al. 2008, 2010; Djanaguiraman et al. 2011). In contrast, ETH treatment promoted the abscission of flowers
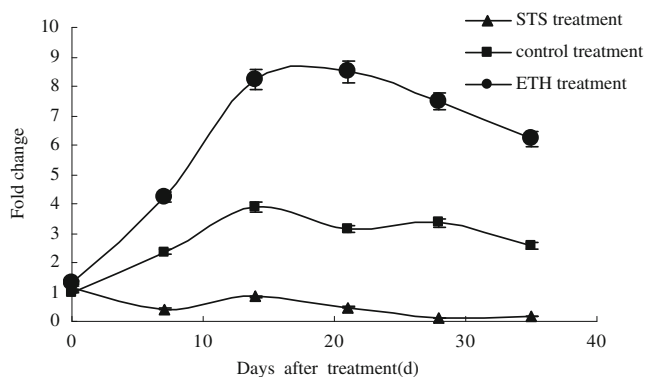
Fig. 5 qRT-PCR analysis of *ACO* (1-aminocyclopropane-1-carboxylate oxidase) gene expression variation after ETH and STS treatments. Expression ratios on different days after STS and ETH treatments are compared with that of the control on day 0
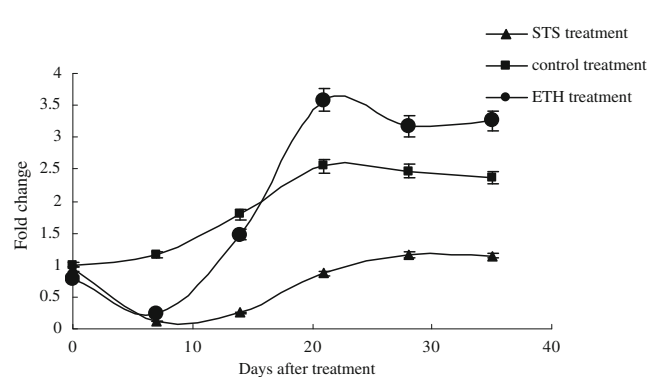

Fig. 6 The qRT-PCR analysis of *ACS* (1-aminocyclopropane-1-carboxylate synthase) gene expression variation after ETH and STS treatments. Expression ratios on different days after ETH and STS treatments are compared with that of the control on day 0

and pods and lateral branch differentiation (Table 2, Fig. 1), suggesting that ethylene plays an important role in early abscission of flowers and pods and in the transition process between the vegetative and reproductive development (Cheng et al. 2010; Chen et al. 2011; Djanaguiraman et al. 2011; Gniazdowska et al. 2010).

Recent studies have highlighted the significance of high-throughput expression data, particularly with the integration of large, diverse data sets, in constructing biochemical and regulatory networks (Hoen et al. 2008; Marioni et al. 2008; Mortazavi et al. 2008; Eveland et al. 2010; Amit et al. 2009). In this study, we analyzed the short-read, sequence-based expression profiles related to ethylene-mediated organ abscission using Illumina's DGE technology. Our results suggest that deep sequencing of 20- to 21-nucleotide DGE tags can be used to successfully establish genome-wide expression profiles in soybean and detect differences in transcript abundance over a broad dynamic range. We identified 11–12 million clean tags from three DGE libraries. Of these, 82.8 % to 83.7 % clean tags could be mapped to unigenes. Results from these expression analyses provided testable hypotheses for resolving which regulatory and biochemical processes contribute to ethylene-regulated soybean reproductive development and abscission. To investigate the functions of the identified ethylene responsive genes, we explored their annotations and functional category in the soybean Genome Annotation Project database (Table 4). Several members of the ethylene receptors gene families, which are known to be induced rapidly by exogenous ethylene (Zhang and Wen 2010; Chervin and Deluc 2010), are listed in Supplement file 4. These results confirmed the reliability of the RNA-seq. Our homogenous expression data sets allowed us to perform counterpart comparisons with ethylene inducers and ethylene inhibitors.

GO analysis and the pathway enrichment analysis of DEGs identified two major functional and process-based categories, which were involved in catalytic activity and response to stimulus, respectively, in the DEGs of control-vs-ETH and control-vs-STS. Pathway enrichment analysis revealed the most significantly affected pathways was the "secondary metabolism, ABA signal and ethylene signal "pathway after ETH treatment. STS treatment affected metabolism of starch and sucrose and signal transduction of auxin, zeatin, brassinosteroid, and salicylic acid. Therefore, this finding implies that the role of ethylene was related to photosynthesis, stress response, carbohydrate transportation, signal transduction and hormone crosstalk (Cheng et al. 2010; Chervin and Deluc 2010; Zhu et al. 2011; Iqbal et al. 2011). In the present study, 17 ethylene-responsive genes were identified as potential key components in complicated ethylene signaling networks. ACO—the key enzyme responsible for ethylene biosynthesis—was up-regulated during soybean reproductive development after ETH treatment, and therefore ethylene promotes ethylene

biosynthesis during soybean reproductive development by positive feedback regulation of ACO (Schaller 2012). The results of qRT-PCR analysis confirmed that the expression of ACO was up-regulated after 14 days of treatment, and this implied that there was a sustained feedback regulation of ethylene. Expression of PP2C was also up-regulated after ETH treatment. The Arabidopsis PP2C enzymes, such as the ABI1/ABI2 PP2Cs, have been identified as central components in abscisic acid (ABA) signal transduction (Ma et al. 2009). An increase in ethylene due to ETH treatment, stress-induced hormones (ABA and ethylene), and some genes associated with stress responses (MAT1, BAHD acyltransferase, CAD) could probably lead to the abscission of flowers and pods in soybean. Furthermore, glucan endo-1, 3-beta-glucosidase 14-like gene, which is involved in cellulose degradation, was significantly up-regulated in the ETH treatment as compared with that in STS treatment (FDR≤0.001), suggesting that stress-induced ethylene is closely related with organ abscission.

The function of up-regulated genes in the STS treatment included genes related to sugar biosynthesis and transport; cell wall metabolism and structure; and synthesis of flower pigment. The expression of Aconitate hydratase, an iron-containing enzyme gene that catalyzes the dehydration of citrate to cis-aconitate (a reaction of significance in the tricarboxylic acid cycle) and a bidirectional sugar transporter SWEET1-like gene were significantly up-regulated (FDR≤ 0.001). Changes in cell wall extensibility appears to be the primary factor regulating segmental growth rates in the root elongation zone (Neumann 1995). Among the 17 ethylene-responded genes, we found 2 non-specific lipid-transfer protein gene and 1 putative cell wall protein gene in the STS treatment, which may play a role in cell-wall metabolism and structure and in suppressing the abscission rate of organs (Nieuwland et al. 2005). Briefly, the expression of genes involved in sugar metabolism and sugar transport in both flowers and pods would contribute to efforts to improve the yield of soybean.

In conclusion, the results of the present study show that inhibition of ethylene could inhibit the abscission of flowers and pods in soybean. Potential target genes regulated by ethylene were identified as follows: ACC-oxidase, PP2Cs, maturation protein gene(MAT1), acetyltransferase, BAHD acyltransferase, CAD, bidirectional sugar transporter SWEET1-like, aconitate hydratas, and Anthocyanidin synthase. These identified genes provided new insights into the molecular mechanism of ethylene-mediated networks regulating abscission and development.

References

Adams DO, Yang SF (1979) Ethylene biosynthesis: identification of 1-aminocyclopropane-1 -carboxylic acid as an intermediate in the conversion of methionine to ethylene. Proc Natl Acad Sci USA 76:170–174

Alonso JM, Ecker JR (2006) Moving forward in reverse: genetic technologies to enable genome-wide phenomic screens in *Arabidopsis*. Nat Rev Genet 7:524–536

Amit I, Garber M, Chevrier N, Leite AP, Donner Y et al (2009) Unbiased reconstruction of a mammalian transcriptional network mediating pathogen responses. Science 326:257–263

Audic S, Claverie JM (1997) The significance of digital gene expression profiles. Genome Res 7:986–995

Benjamini Y, Yekutieli D (2001) The control of the false discovery rate in multiple testing under dependency. Ann Stat 29:1165–1188

Chen MK, Hsu WH, Lee PF, Thiruvengadam M, Chen HI et al (2011) The MADS box gene, FOREVER YOUNG FLOWER, acts as a repressor controlling floral organ senescence and abscission in *Arabidopsis*. Plant J 68:168–185

Cheng YQ, Yang J, An LJ, Liu JF, Chen ZW (2008) Effects of ethylene on yield and floral organ development in soybean (*Glycine max*). J Zhejiang Univ (Agric Life Sci) 34:540–545

Cheng YQ, Zhao GL, Liu JF, Chen ZW, Zhang WW (2010) Effects of ethylene inhibitor and promoter on photosynthetic characteristics of soybean (*Glycine max*) seedling leaves. J Zhejiang Univ (Agric Life Sci) 36:419–426

Chervin C, Deluc L (2010) Ethylene signaling receptors and transcription factors over the grape berry development: gene expression profiling. Vitis 49:129–136

Cloonan N, Grimmond SM (2008) Transcriptome content and dynamics at single-nucleotide resolution. Genome Biol 9:234

Djanaguiraman M, Prasad PVV, Al-Khatib K (2011) Ethylene perception inhibitor 1-MCP decreases oxidative damage of leaves through enhanced antioxidant defense mechanisms in soybean plants grown under high temperature stress. Environ Exp Bot 71:215–223

Dong CH, Jang M, Scharein B, Malach A, Rivarola M et al (2010) Molecular association of the *Arabidopsis* ETR1 Ethylene receptor and a regulator of ethylene signaling, RTE1. J Biol Chem 285:40706–40713

Eveland A, Satoh-Nagasawa N, Goldshmidt A, Meyer S, Beatty M et al (2010) Digital gene expression signatures for maize development. Plant Physiol 154:1024–1039

Fehr WR, Caviness CF, Burmood DT, Pennington JS (1971) Stage of development descriptions for soybeans, glycine max. (L). Merrill. Fehr & Caviness et al. Crop Sci 11:929–931

Gniazdowska A, Krasuska U, Czajkowska K, Bogatek R (2010) Nitric oxide, hydrogen cyanide and ethylene are required in the control of germination and undisturbed development of young apple seedlings. Plant Growth Regul 61:75–84

Gu Z, Steinmetz LM, Gu X, Scharfe C, Davis RW et al (2003) Role of duplicate genes in genetic robustness against null mutations. Nature 421:63–66

Hamilton AJ, Bouzayen M, Grierson D (1991) Identification of a tomato gene for the ethylene-forming enzyme by expression in yeast. Proc Natl Acad Sci USA 88:7434–7437

Heindl JC, Brun WA (1984) Patterns of reproductive abscission, seed yield, and yield components in soybean. Crop Sci 24:542–545

Hirayama T, Shinozaki K (2010) Research on plant abiotic stress responses in the post-genome era: past, present and future. Plant J 61:1041–1052

Hoen PA, Ariyurek Y, Thygesen HH, Vreugdenhil E, Vossen RH et al (2008) Deep sequencing-based expression analysis shows major advances in robustness, resolution and interlab portability over five microarray platforms. Nucleic Acids Res 36:e141

Iqbal N, Nazar R, Syeed S, Masood A, Khan NA (2011) Exogenously-sourced ethylene increases stomatal conductance, photosynthesis, and growth under optimal and deficient nitrogen fertilization in mustard. J Exp Bot 62:4955–4963

Kanehisa M, Araki M, Goto S, Hattori M, Hirakawa M et al (2008) KEGG for linking genomes to life and the environment. Nucleic Acids Res 36:480–484

Kubis S, Patel R, Combe J, Bedard J, Kovacheva S et al (2004) Functional specialization amongst the *Arabidopsis* Toc159 family of chloroplast protein import receptors. Plant Cell 16:2059–2077

Li H, Ruan J, Durbin R (2008) Mapping short DNA sequencing reads and calling variants using mapping quality scores. Genome Res 18:1851–1858

Li RQ, Yu C, Li YR, Lam TW, Yiu SM et al (2009) SOAP2: An improved ultrafast tool for short read alignment. Bioinformatics 25:1966–1967

Lin ZF, Zhong SL, Grierson D (2009) Recent advances in ethylene research. J Exp Bot 60:3311–3336

Lister R, O'Malley RC, Tonti-Filippini J, Gregory BD, Berry CC et al (2008) Highly integrated single-base resolution maps of the epigenome in *Arabidopsis*. Cell 133:523–536

Lorbiecke R, Sauter M (1999) Adventitious root growth and cell cycle induction in deepwater rice (*Oryza sativa* L.). Plant Physiol 119:21–29

Ma Y, Szostkiewicz I, Korte A, Moes D, Yang Y et al (2009) Regulators of PP2C phosphatase activity function as abscisic acid sensors. Science 324:1064–1068

Marioni JC, Mason CE, Mane SM, Stephens M, Gilad Y (2008) RNA-seq: an assessment of technical reproducibility and comparison with gene expression arrays. Genome Res 18:1509–1517

Mortazavi A, Williams BA, McCue K, Schaeffer L, Wold B (2008) Mapping and quantifying mammalian transcriptomes by RNA-Seq. Nat Methods 5:621–628

Nambeesan S, AbuQamar S, Laluk K, Mattoo AK, Mickelbart MV et al (2012) Polyamines attenuate ethylene-mediated defense responses to abrogate resistance to *Botrytis cinerea* in tomato. Plant Physiol 158:1034–1045

Neumann PM (1995) The role of cell wall adjustment in plant resistance to water deficits (review and interpretation). Crop Sci 35:1258–1266

Nieuwland J, Feron R, Huisman BAH, Fasolino A, Hilbers CW et al (2005) Lipid transfer proteins enhance cell wall extension in tobacco. Plant Cell 17:2009–2019

Pasek S, Risler JL, Brezellec P (2006) The role of domain redundancy in genetic robustness against null mutations. J Mol Biol 362:184–191

Rylott PD, Smith ML (1990) Effects of applied plant growth substances on pod set in broad beans (*Vicia faba* var. Major). J Agric Sci Camb 114:41–47

Sato T, Theologis A (1989) Cloning the mRNA encoding 1-aminocyclopropane-1- carboxylate synthase, the key enzyme for ethylene biosynthesis in plants. Proc Natl Acad Sci USA 86:6621–6625

Schaller GE (2012) Ethylene and the regulation of plant development. BMC Biol 10:9. doi:10.1186/1741-7007-10-9

Singh AP, Tripathi SK, Nath P, Sane AP (2011) Petal abscission in rose is associated with the differential expression of two ethylene-responsive xyloglucan endotransglucosylase/hydrolase genes, RbXTH1 and RbXTH2. J Exp Bot 62:5091–5103

Stangeland B, Nestestog R, Grini PE, Skrbo N, Berg A et al (2005) Molecular analysis of *Arabidopsis* endosperm and embryo promoter trap lines: reporter-gene expression can result from T-DNA insertions in antisense orientation, in introns and in intergenic regions, in addition to sense insertion at the 5′ end of genes. J Exp Bot 56:2495–2505

Trivellini A, Ferrante A, Vernieri P, Serra G (2011) Effects of promoters and inhibitors of ethylene and ABA on flower senescence of *Hibiscus rosa-sinensis* L. J Plant Growth Regul 30:175–184

Wang Z, Gerstein M, Snyder M (2009) RNA–Seq: a revolutionary tool for transcriptomics. Nat Rev Genet 10:57–63

Wiebold W, Ashley D, Boerma HR (1981) Reproductive abscission levels and patterns for eleven determinate soybean cultivars. Agron J 73:43–46

Wilhelm BT, Marguerat S, Watt S, Schubert F, Wood V et al (2008) Dynamic repertoire of a eukaryotic transcriptome surveyed at single-nucleotide resolution. Nature 453:1239–1243

Xue JQ, Li YH, Tan H, Yang F, Ma N et al (2008) Expression of ethylene biosynthetic and receptor genes in rose floral tissues during ethylene-enhanced flower opening. J Exp Bot 59:2161–2169

Xue J, Bao YY, Li BL, Cheng YB, Peng ZY et al (2010) Transcriptome analysis of the brown planthopper Nilaparvata lugens. PLoS One 5:e14233

Zhang W, Wen CK (2010) Preparation of ethylene gas and comparison of ethylene responses induced by ethylene, ACC and ethephon. Plant Physiol Biochem 48:45–53

Zhu H, Dardick CD, Beers EP, Callanhan AM, Xia R et al (2011) Transcriptomics of shading-induced and NAA induced abscission in apple (Malus domestica) reveals a shared pathway involving reduced photosynthesis, alterations in carbohydrate transport and signaling and hormone crosstalk. BMC Plant Biology 11:138